Radiation Pattern Analysis of Reflector Antennas Using CAD Model-Based Physical Optics Method

ZHEN LEI

School of Construction Machinary, Chang'an University, Xi'an 710064,China
The 39th Research Institute of China Electronics Technology Group Corporation, Xi'an 710065, China
Shaanxi Key Laboratory of Antenna and Control Technology, Xi'an 710065, China

e-mail: leizhen__2006@163.com

ABSTRACT Radiation pattern analysis is important in reflector antenna design. Mesh model based physical optics method is widely used in such circumstance. There are always geometric errors between mesh model and CAD model, and the analysis will be subjected to geometric noise, which will ultimately deteriorate its accuracy. In this paper, such analysis is implemented directly with the CAD model. The reflector expressed by Non-Uniform Rational B-Spline (NURBS) is firstly refined by NURBS operation. It does not change the original shape, but divides it into small parametric areas, named as elements. The physical optics integration performs in each element with Gauss quadrature, and finally superimposes to obtain the radiation pattern of the antenna. Several examples show that this method is effective and efficient, and it will lay a foundation for antenna shape optimization with CAD models.

INDEX TERMS Radiation pattern analysis, reflector antenna, CAD model, physical optics, NURBS.

I. INTRODUCTION

Large reflector antennas are widely used in radio astronomy, satellite communications, deep space exploration, etc. because of their high gain, low sidelobe and narrow beam characteristics [1], [2], they are also less expensive than other antenna forms.

Many techniques are currently available for radiation performance analysis of reflector antennas, the frequently used methods are geometric optics (GO) and physical optics (PO). The former is based on the principle of geometric optics (GO), which is suitable for large antenna systems where the wavelength of the electromagnetic wave is relatively very short. GO has ray caustic problems in the main-beam direction when used for parabolic antennas. The latter is very accurate in the main beam and the first few side-lobe regions [3], it is sufficient for finding the antenna gain or the near-in side-lobes [4]. Other methods, like Moment Method (MoM) [5], Finite Element Method (FEM) [6], Geometrical Theory of Diffraction (GTD) [7], Uniform Theory of Diffraction (UTD) [8] and Physical Theory of Diffraction (PTD) [9] are also used in the antenna simulations. They have been incorporated into the commercial electromagnetic simulation

The associate editor coordinating the review of this manuscript and approving it for publication was Kwok L. Chung .
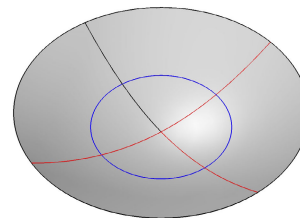

FIGURE 1. The NURBS surface.

software, e.g. FEKO, Grasp, and are vastly adopted in the design of large reflect antennas.

The antenna reflector is described by NURBS in CAD modeling. This is the standard data exchange format for CAD systems, which will also drive the subsequent antenna panel fabrication. At present, the above surface is converted into a mesh model for simulation, and then physical optics calculation is performed on it. There always exist geometric errors between the mesh model and the original NURBS surface, as shown in Fig. 1 and Fig. 2. This artificially introduced error will decrease the simulation accuracy. As the number of elements increases, the geometric error decreases, but the computing burden will increase. At high frequencies, the reflector has higher requirements on the surface accuracy. It limits the
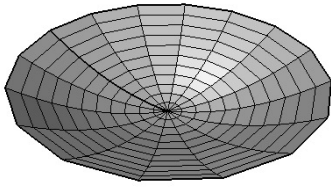
FIGURE 2. The quadrilateral facets approximated surface.

maximum operating frequency of the reflector antenna [2]. The above geometric error problem becomes more severe, much more elements should be used in simulation. For large antennas, the computing burden might increase to a level that the normal computer cannot afford.

Performing the physical optics calculation directly on the CAD model is very attractive, since there will be no geometric error. There are some relevant studies on this topic. J. Perez is the pioneer who proposed a method for evaluating the radar cross section (RCS) based on NURBS modelling in 1994 [10], [11]. Their method was verified by analysing the RCS of cylindrical surface, conical surface and spherical cone combination, it gave good results. M. Domingo et al. improved the above method in 1995 by introducing shadow region recognition on NURBS model. They also developed software RANUBS, which is based on PO. Basic algorithms, the second-order field processing and occlusion judgement are detailed in [12]. PO combined with a shape reconstruction procedure, has also been employed for studying the inverse scattering problem for the reconstruction of three-dimensional electrically large conducting NURBS patches [13]. The PO on trimmed NURBS surface is studied in [14]. The above methods basically focus on RCS calculation of the structures.

In this paper, the physical optics method is implemented directly with the CAD model of the antenna to perform a fast evaluation of its radiation pattern. First, the model of the reflector is refined by NURBS operation, and the original NURBS is divided into small parametric areas, which are named as elements. This operation does not change the shape of the initial NURBS. Then, Gauss quadrature integration is implemented in each element and finally sums up to obtain the radiation field.

The article is organized as follows. In theoretical part, the NURBS description of the reflector and the radiation pattern evaluation with PO method are presented. In numerical results section, two examples on pattern analysis of rotationally symmetric reflector antennas are given to verify the method. Various results and comparisons are reported in this section. Finally, a conclusion is given at the end of the article.

II. THEORETICAL PART
A. NURBS DESCRIPTION OF THE REFLECTOR
The antenna reflector is normally described by NURBS in CAD model. A NURBS curve is a piecewise polynomial curve based on B-spline, which is a linear combination of
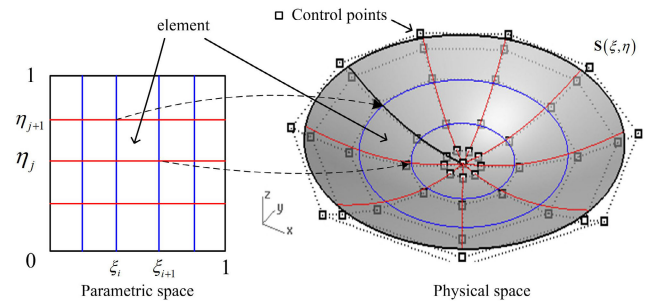

FIGURE 3. The NURBS surface, the elements and control points.

B-spline basis functions. The combination coefficients are called control points. B-spline basis functions are defined over a non-decreasing real number set. The set $\Xi = \{\xi_1, \xi_2, \cdots, \xi_{p+n+1}\}$ is called a knot vector, p and n indicate the order of the curve and the number of control points respectively. The whole interval of the set is called a patch. A detailed introduction about NURBS can be found in [15].

The B-spline basis functions are defined recursively as

$$N_{i,0}(\xi) = \begin{cases} 1 & if\ \xi_i \le \xi < \xi_{i+1} \\ 0 & otherwise, \end{cases} \tag{1}$$

$$N_{i,p}(\xi) = \frac{\xi - \xi_i}{\xi_{i+p} - \xi_i} N_{i,p-1}(\xi) + \frac{\xi_{i+p+1} - \xi}{\xi_{i+p+1} - \xi_{i+1}} N_{i+1,p-1}(\xi). \tag{2}$$

The NURBS surface can be expressed as follows

$$\mathbf{S}(\xi, \eta) = \sum_{i=1}^{n} \sum_{j=1}^{m} \mathbf{P}_{i,j} R_{i,j}^{p,q}(\xi, \eta). \tag{3}$$

Here, $\mathbf{P}_{i,j}$ denotes the three dimensional coordinate of the control point, $R_{i,j}^{p,q}$ are bivariable scalar functions named as basis functions,

$$R_{i,j}^{p,q}(\xi, \eta) = \frac{N_{i,p}(\xi) N_{j,q}(\eta) w_{i,j}}{\sum_{k=1}^{n} \sum_{l=1}^{m} N_{k,p}(\xi) N_{l,q}(\eta) w_{k,l}}. \tag{4}$$

Fig. 3 shows a NURBS patch example. The shape can be manipulated by moving the control points. The closure of Ξ constitutes the parametric space, which normally spans from 0 to 1. Each non-empty interval corresponds to a segment of the curve, and can be viewed as an "element" in 1D case, like what in the finite element analysis. In 2D case, the parametric space of the whole patch is $[0, 1]^2$, a 2D element is the area encircled by the parameter isolines, its corresponding parametric space is $[\xi_i, \xi_{i+1}] \otimes [\eta_j, \eta_{j+1}]$, depicted in Fig. 3.

The elements are created by the NURBS knot insertion [15], which is an operation that can insert more knots into the initial parametric interval while keeping the shape unchanged. With its help, the initial surface can be dived into lots of small elements both in parametric space and in physical space without losing any geometric accuracy.
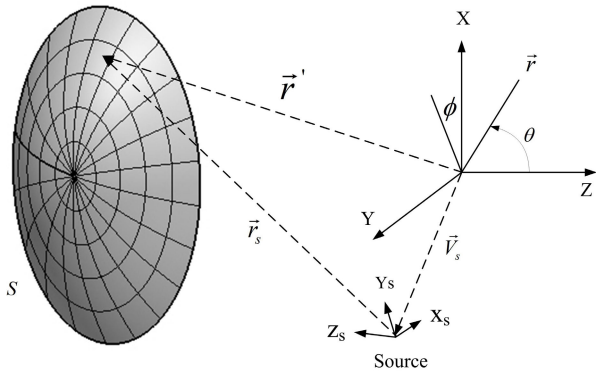
FIGURE 4. A reflector antenna illuminated by an arbitrarily located source.

This is very different from what in the traditional FEM analysis, where the creation of the mesh will inevitably induce geometrical accuracy lose, since facets are used there to approximate the initial NURBS, their mathematical backgrounds are different, the later cannot exactly express the former, approximation error always exists no matter how fine the meshes are.

The antenna reflector in the CAD model is expressed by the NURBS, shown in Fig. 1. It is a paraboloid expressed by bicubic NURBS. With the pre-mentioned nurbs insertion operation, it can be divided into a lot of pieces both in parametric space and in physical space for the convenience of implementing the physical optics integral in the antenna reflector, shown in Fig. 3. For comparison, a traditionally used quadrilateral mesh is shown in Fig. 2, geometrical error can be seen apparently, it will cause facet noise in electromagnetic simulation.

B. RADIATION PATTERN ANALYSIS WITH PO

The geometry of a reflector antenna with an arbitrarily source is shown in Fig. 4. The Physical Optics formulae are expressed as [16], [17]

$$\vec{E}(\theta, \phi) = -jk\eta \frac{e^{-jkr}}{4\pi r}\left(\bar{\bar{I}} - \hat{r}\hat{r}\right) \cdot \vec{T}, \tag{5}$$

$$\vec{T}(\theta, \phi) = \int_S \vec{J}(\vec{r}')e^{-jk\vec{r}\cdot\hat{r}}ds, \tag{6}$$

$$\vec{J}(\vec{r}') = 2\hat{n} \times \vec{H}^{inc}(\vec{r}'). \tag{7}$$

Here, $j = \sqrt{-1}$, $k = 2\pi/\lambda$, λ is the wavelength, $\eta = 120\pi$ is the free-space wave impedance, $\hat{n}$ denotes the outward unit normal vector of the reflector surface as depicted in Fig. 4, $\hat{r}$ is a unit vector in the observation direction, $\hat{r}'$ denotes any point on the reflector **S**, and $\vec{V}_s$ denotes the spatial coordinates of electromagnetic source in the global *XYZ* Cartesian coordinate system, $\vec{r}_s$ denotes the spatial coordinates of a point on the reflector S in the source local coordinate system $x_s y_s z_s$.

The reflector is expressed by NURBS, thus

$$\vec{r}' = \mathbf{S}(\xi, \eta) = \sum_{i=1}^{n}\sum_{j=1}^{m}\mathbf{P}_{i,j}R_{i,j}^{p,q}(\xi, \eta). \tag{8}$$

And $\hat{n}$ can be obtained as

$$\hat{n} = \frac{\vec{n}}{\|\vec{n}\|}. \tag{9}$$

$$\vec{n} = \mathbf{S}_{,\xi} \times \mathbf{S}_{,\eta} \tag{10}$$

$$\mathbf{S}_{,\xi} = \partial\mathbf{S}/\partial\xi = \sum_{i=1}^{n}\sum_{j=1}^{m}\mathbf{P}_{i,j}\frac{\partial R_{i,j}^{p,q}(\xi, \eta)}{\partial\xi} \tag{11}$$

$$\mathbf{S}_{,\eta} = \partial\mathbf{S}/\partial\eta = \sum_{i=1}^{n}\sum_{j=1}^{m}\mathbf{P}_{i,j}\frac{\partial R_{i,j}^{p,q}(\xi, \eta)}{\partial\eta} \tag{12}$$

The algorithms for evaluating the derivatives of the NURBS basis functions can be found in many CAD books [15]. The incident electromagnetic wave emitting form the source is normally formulated in the source local cylindrical coordinate system as following,

$$\vec{E}_s(\vec{r}_s) = \left(U(\theta_s, \phi_s)\hat{\theta}_s + V(\theta_s, \phi_s)\hat{\phi}_s\right)\frac{e^{-jkr_s}}{4\pi r_s}, \tag{13}$$

$$\vec{H}_s(\vec{r}_s) = \frac{1}{\eta}\left(-V(\theta_s, \phi_s)\hat{\theta}_s + U(\theta_s, \phi_s)\hat{\phi}_s\right)\frac{e^{-jkr_s}}{4\pi r_s}. \tag{14}$$

Here, functions U and V decide the primary pattern of the feed. The footnote s indicates those variables relate to the source coordinate system, depicted in Fig. 4, $\vec{r}_s$ denotes a point on the reflector S in the local coordinate system,

$$\vec{r}_s = \vec{r}' - \vec{V}_s. \tag{15}$$

And $r_s = \|\vec{r}_s\|$, θ_s and ϕ_s are components of $\vec{r}_s$ in local spherical coordinates axes $\hat{\theta}_s$ and $\hat{\phi}_s$ direction respectively.

Thus the incident wave on the reflector is

$$\vec{H}^{inc}(\vec{r}') = \vec{H}_s(\vec{r}_s). \tag{16}$$

The integration in (6) will be carried out on NURBS surface **S**, since NURBS has natural parametric space, it can be formulated as

$$\vec{T}(\theta, \phi) = \iint_{[0,1]^2} \vec{J}(\vec{r}')e^{-jk\vec{r}'\cdot\hat{r}}\|\vec{n}\|d\xi d\eta. \tag{17}$$

Here, $\|\vec{n}\|$ is the Jacobi of the NURBS surface, it has been calculated by (10). Gauss quadrature is adopted here, shown in Fig.5. It will be implemented in each element, and then sums up, formulated as

$$\vec{T}(\theta, \phi) = \sum_{j=1}^{nelem}\sum_{i=1}^{gn^2}\vec{J}(\vec{r}')e^{-jk\vec{r}'\cdot\hat{r}}\|\vec{n}\|L_i. \tag{18}$$

Here, gn^2 indicates the number of Gauss points in each element, L_i is the integral weight, *nelem* denotes the total number of elements. The quadrature accuracy depends on *gn* and *nelem*, more elements and quadrature points will give better accuracy, they can be controlled by the users.

With the reflector shape, the location, the orientation of the feed and its primary pattern formulations, the secondary electromagnetic wave of the antenna can be calculated, and its radiation pattern can thus be obtained. CAD model is used directly here, it avoids the geometrical approximations which will introduce errors in the commonly used
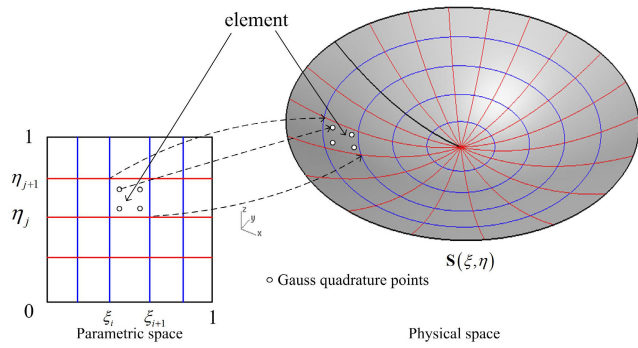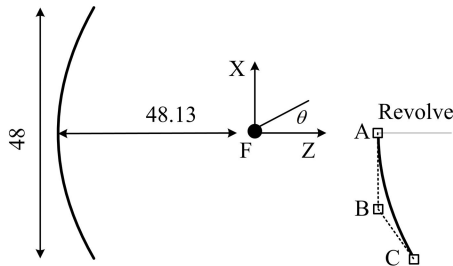
FIGURE 5. The numerical integration of PO on NURBS.

FIGURE 7. The NURBS expressed paraboloid.

FIGURE 6. The geometry of the paraboloid antenna.
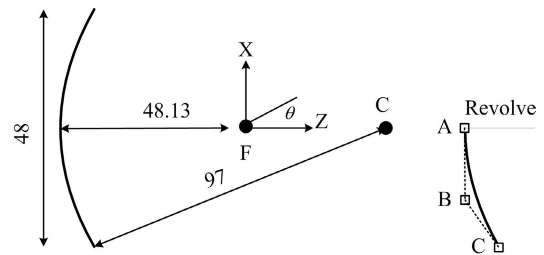
FIGURE 8. The geometry of the spherical antenna.

model discretization, and thus accuracy improvements can be expected. The process needs basic algorithms of the NURBS, which are massively studied in the CAD and mechanical engineering research. They are very mature and fast, not to mention that there are many items used repeatedly and all the calculations can be carried out with vector operations. The feasibility and efficiency of the method can be guaranteed.

III. NUMERICAL RESULTS AND DISCUSSIONS

In this part, two examples will be given to verify the effectiveness of the approach. The reflectors are standard conical surfaces. They can be exactly expressed by NURBS. Their radiation patterns will be evaluated. Those examples have appeared in paper [17], the problem setup is fully reproduced here so that fair comparisons can be made and reasonable conclusions can be obtained.

A. PARABOLOID REFLECTOR

The first example we consider parabolic reflector [17], its geometry is shown in Fig. 6 and Fig. 7. The shape is obtained by revolving a NURBS expressed partial parabolic along z axis. The feed is located at the focal point with a $\mathbf{y_s}$-polarized radiated $\mathbf{E}$ field which produces a -18.5dB edge taper. The far-field pattern of the feed as defined in (14) is

$$\begin{cases} V\left(\theta_s, \phi_s\right) = -\cos\left(\phi_s\right)\cos^q\left(\theta_s\right) \\ U\left(\theta_s, \phi_s\right) = -\sin\left(\phi_s\right)\cos^q\left(\theta_s\right), \end{cases} \quad (19)$$

where $q = 17.1094$.

TABLE 1. The geometric coefficients of the parabolic antenna.

Parabolic Reflector	Feed
Knot vector	Location
$\Xi = \{0, 0, 0, 1, 1, 1\}$	$\vec{V}_s = [0, 0, 0]$
Control point coordinate	Orientation
A [0, 0, -48.130], $w_a = 1$	$\vec{x}_s = [1, 0, 0]$
B [-12, 0, -48.130], $w_b = 1$	$\vec{y}_s = [0, -1, 0]$
C [-24, 0, -45.138], $w_c = 1$	$\vec{z}_s = [0, 0, -1]$

The location and orientation of the feed are defined by its local coordinate system. The coefficients are listed in Table 1. It should be noted that there are many parametrizations for the same parabolic. We use cubic NURBS with coefficients shown in that table. All the weight of the control points are 1, it is in fact a B-spline here.

The wavelength λ is set to 1. The initial reflector only consists 4 elements as shown in Fig. 7. To obtain a reasonable result, it is refined into $6 \times 20 = 120$ elements as shown in Fig. 9. Three-point Gauss quadrature is adopted, and there are 9 quadrature points in each element. The radiation pattern is shown in Fig. 10, the results from [17] are also depicted. They match each other well. Fig. 11 shows the results when the number of quadrature points is also chosen as $gn = 2$ (4 points in an element) and $gn = 4$ (16 points in an element). It can be seen that the result improves as the number of quadrature points increases, results from $gn = 3$ and $gn = 4$ are almost the same, results from $gn = 2$ are slightly different with the others, shown in the zoomed region. We also study the cases where different amount of flat facets are used to approximate the reflector.
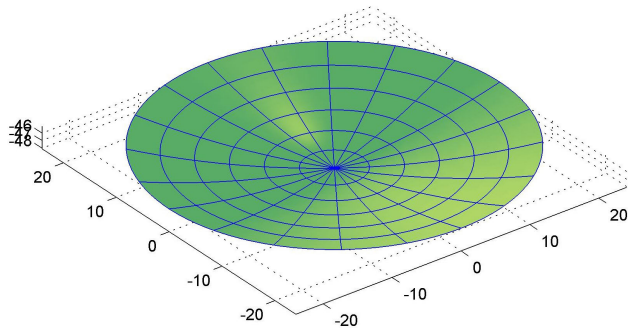
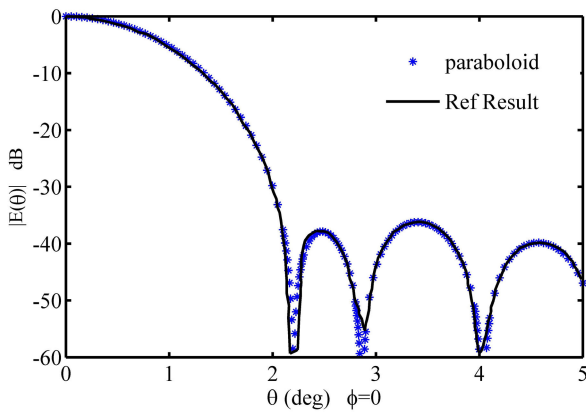**FIGURE 9.** The fine meshed paraboloid.

FIGURE 10. The radiation pattern of the paraboloid antenna and its comparison with results from [17].
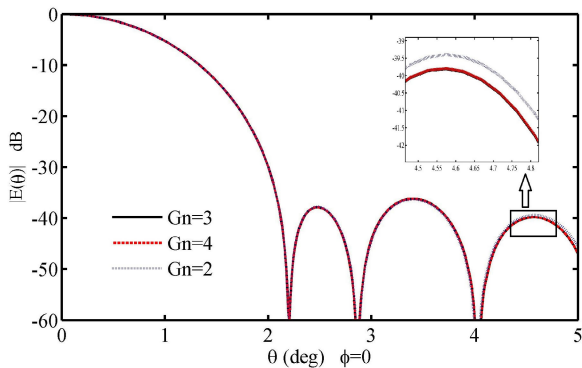

FIGURE 11. The radiation patterns of the paraboloid antenna with *Gn* points Gauss quadrature.

Fig. 12 shows the results from faceted meshes. The results converge as the number of facets increases. However it behaves worse than our method, the results from 1920 facets are merely comparable with our 120 elements results. It indicates that our method is at least 16 times faster than the flat facet method in this example.

B. SPHERICAL REFLECTOR

The second example is a spherical reflector [17] with its geometry shown in Fig. 8. The feed is located at the optimum point for focusing [17] and has a $\mathbf{y_s}$-polarized **E** field which produces a -18.5dB edge taper. The far-field pattern of the
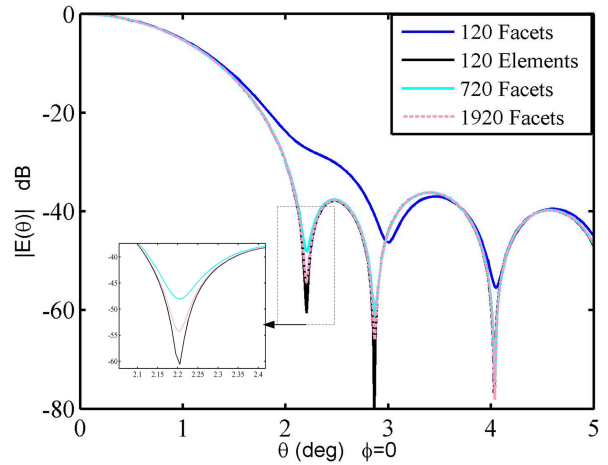

FIGURE 12. The radiation patterns of the paraboloid antenna with different number of flat facet meshes.

TABLE 2. The geometric coefficients of the spherical antenna.

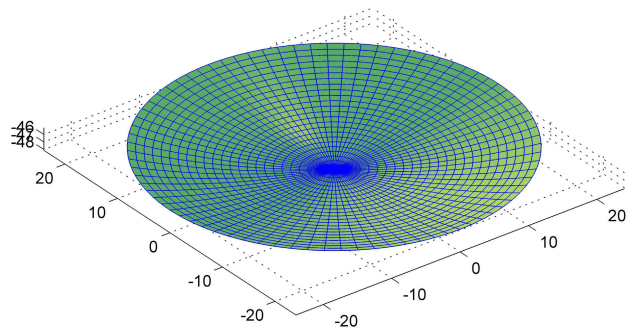| Spherical Reflector	Feed
Knot vector	Location
$\Xi = \{0, 0, 0, 1, 1, 1\}$	$\vec{V}_s = [0, 0, 0]$
Control point coordinate	Orientation
A $[0, 0, -48.13]$, $w_a = 1$	$\vec{x}_s = [1, 0, 0]$
B $[-12.190, 0, -48.130]$, $w_b = 0.992$	$\vec{y}_s = [0, -1, 0]$
C $[-24, 0, -45.114]$, $w_c = 1$	$\vec{z}_s = [0, 0, -1]$

FIGURE 13. Spherical reflector meshed with 1920 elements.

feed is given in (19) and $q = 17.0933$. The shape is also obtained from revolving. Its geometric coefficients are listed in Table 2. Here the weight of control point B is not 1. It is also a shallow curved surface. The 3*D* shape resembles the paraboloid shown in Fig. 7.

The wavelength λ is set to 1. The initial revolved reflector also has 4 elements. The shape is refined to 120 elements for calculation. Three-point Gauss quadrature is also adopted. The radiation pattern is shown in Fig. 15, it also includes the results from [17]. It can be seen from the comparison that pretty good result can be obtained with only 120 elements. We also study the cases where the geometry is refined into 1920 and 3600 elements, depicted in Fig. 13 and Fig. 14. Their corresponding results are shown in Fig. 16. All results match well, it proves the convergence of the method. Fig. 17 shows the result with 3600 elements as $\lambda = 0.5$, it can be
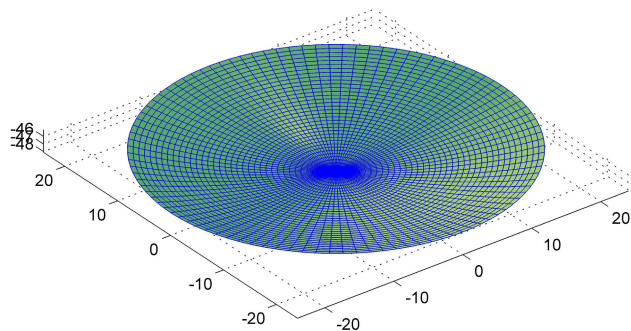
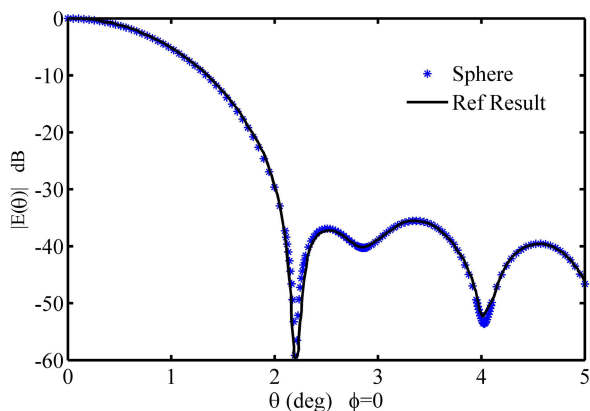**FIGURE 14.** Spherical reflector meshed with 3600 elements.

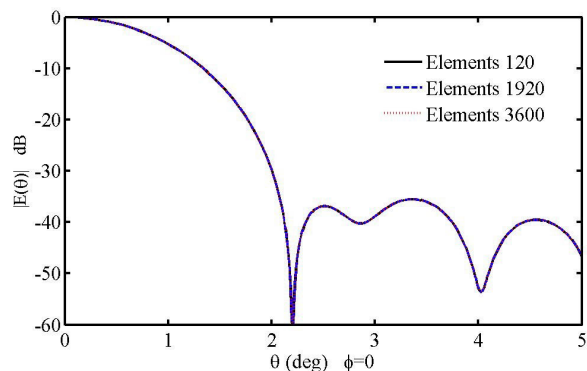**FIGURE 15.** The radiation pattern of the spherical antenna and its comparison with results from [17].

FIGURE 16. The radiation pattern of the spherical antenna obtained from different mesh densities.

FIGURE 17. The radiation pattern of the spherical antenna as lamda = 1 and lamda = 0.5 with 3600 elements.

IV. CONCLUSION

This paper presents a CAD model based method for evaluating the antenna radiation pattern. The NURBS and its related operations are used to express the antenna reflector and create the geometrically exact mesh, there is no geometrical difference between the CAD model and the mesh, and thus no geometrical error interfere the electromagnetic evaluation. The physical optics method is implemented under the NURBS framework, the formulations become concise and can be easily implemented with the matured NURBS algorithms. Examples show that the method is exact and efficient. It can be used in the shape design of the reflectors for the electromagnetic criteria, since the update of CAD model only needs simple NURBS refinement operation. It avoids the cumbersome mesh creation process in the traditional analysis. The final shape obtained will be formulated by NURBS, which can be directly used in manufacturing.

REFERENCES

[1] S. K. Sharma, *Handbook of Reflector Antennas and Feed Systems: Theory and Design of Reflectors*, vol. 1. Norwood, MA, USA: Artech House, 2013.
[2] Y. Rahmat-Samii and R. Haupt, "Reflector antenna developments: A perspective on the past, present and future," *IEEE Antennas Propag. Mag.*, vol. 57, no. 2, pp. 85–95, Apr. 2015.
[3] G. Cortes-Medellin and P. F. Goldsmith, "Analysis of active surface reflector antenna for a large millimeter wave radio telescope," *IEEE Trans. Antennas Propag.*, vol. 42, no. 2, pp. 176–183, Feb. 1994.
[4] D.-W. Duan and Y. Rahmat-Samii, "A generalized diffraction synthesis technique for high performance reflector antennas," *IEEE Trans. Antennas Propag.*, vol. 43, no. 1, pp. 27–40, Jan. 1995.
[5] R. F. Harrington, *Field Computation By Moment Method*. London, U.K.: Macmilan, 1968.
[6] J. Jin, *The Finite Element Method in Electromagnetics*. New York, NY, USA: Wiley, 2002.
[7] V. A. Borovikov and B. E. Kinber, *Geometrical Theory of Diffraction*. London, U.K.: Institution of Electrical Engineers, 1994.
[8] R. G. Kouyoumjian and P. H. Pathak, "A uniform geometrical theory of diffraction for an edge in a perfectly conducting surface," *Proc. IEEE*, vol. 62, no. 11, pp. 1448–1461, Nov. 1974.
[9] S.-W. Lee, "Comparison of uniform asymptotic theory and Ufimtsev's theory of electromagnetic edge diffraction," *IEEE Trans. Antennas Propag.*, vol. AP-25, no. 2, pp. 162–170, Mar. 1977.
[10] J. Perez and M. F. Catedra, "RCS of electrically large targets modelled with NURBS surfaces," *Electron. Lett.*, vol. 28, no. 12, pp. 1119–1121, Jun. 1992.
[11] J. Perez and M. F. Catedra, "Application of physical optics to the RCS computation of bodies modeled with NURBS surfaces," *IEEE Trans. Antennas Propag.*, vol. 42, no. 10, pp. 1404–1411, Oct. 1994.

seen that the main lobe is narrowed, which is consistent with the theoretical analysis.

The calculation time for the case of 3600 elements is only 13.7s using a laptop with two cores 2.4GHz CPU and 8G memories. The algorithm is efficient, since it is fully under the NURBS framework. The formulations are concise, many intermediate variables are evaluated one time but are reused many times. Most of the time is spent on element quadrature, it is easy to change the algorithm into paralleled form to further improve the efficiency.
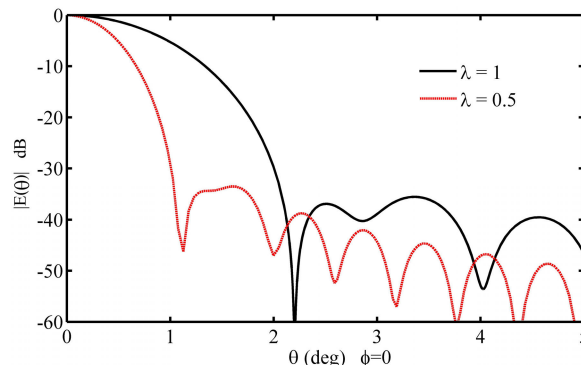
[12] M. Domingo, F. Rivas, J. Perez, R. P. Torres, and M. F. Catedra, "Computation of the RCS of complex bodies modeled using NURBS surfaces," *IEEE Antennas Propag. Mag.*, vol. 37, no. 6, pp. 36–47, Dec. 1995.

[13] A. Saeedfar and K. Barkeshli, "Shape reconstruction of three-dimensional conducting curved plates using physical optics, NURBS modeling, and genetic algorithm," *IEEE Trans. Antennas Propag.*, vol. 54, no. 9, pp. 2497–2507, Sep. 2006.

[14] J. Yan, J. Hu, and Z. Nie, "Calculation of the physical optics scattering by trimmed nurbs surfaces," *IEEE Antennas Wireless Propag. Lett.*, vol. 13, no. 1, pp. 1640–1643, 2015.

[15] L. Piegl and W. Tiller, *The NURBS Book*. Berlin, Germany: Springer, 1997.

[16] Y. Rahmat-Samii, "A comparison between GO/aperture-field and physical-optics methods of offset reflectors," *IEEE Trans. Antennas Propag.*, vol. AP-32, no. 3, pp. 301–306, Mar. 1984.

[17] Y. Rahmat-Samii and V. Galindo-Israel, "Shaped reflector antenna analysis using the Jacobi-Bessel series," *IEEE Trans. Antennas Propag.*, vol. AP-28, no. 4, pp. 425–435, Jul. 1980.
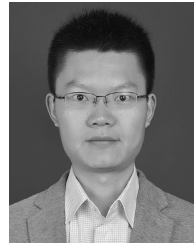
ZHEN LEI was born in Nanyang, China, in 1988. He received the B.S. and M.S. degrees in mechatronics engineering from the Xi'an University of Electronic Science and Technology (Xidian University), China, in 2012, and the Ph.D. degree in mechanics from the Ecole Centrale de Lyon (Lyon University), France, in 2016.

From 2016 to 2017, he was an Assistant Professor with the Mechanical Engineering Department, Chang'an University, where he has been an Associate Professor, since 2018. Since 2019, he has also been a part-time Senior Research Engineer with the 39th Research Institute of China Electronics Technology Group Corporation and the Shaanxi Key Laboratory of Antenna and Control Technology. His research interests include multiphysics analysis with CAD model, computational mechanics and electromagnetics, design optimization, and their application in antenna engineering.

● ● ●